

# In situ ellipsometric control of growth processes of ZnTe and CdTe buffer layers in technology of molecular beam epitaxy of mercury cadmium telluride

© V.A. Shvets<sup>1,2</sup>, D.V. Marin<sup>1,2</sup>, M.V. Yakushev<sup>1</sup>, S.V. Rykhlytskii<sup>1</sup>

<sup>1</sup> Rzhanov Institute of Semiconductor Physics, Siberian Branch, Russian Academy of Sciences, 630090 Novosibirsk, Russia

<sup>2</sup> Novosibirsk State University, 630090 Novosibirsk, Russia

E-mail: basil5353@mail.ru

Received June 15, 2023

Revised July 28, 2023

Accepted August 3, 2023

The problems of *in situ* ellipsometric control during the growth of ZnTe and CdTe buffer layers intended for cadmium-mercury-tellurium epitaxy are considered. It has been established that for 20 nm ZnTe layers the spectral dependences of the optical constants near the absorption edge are smoothed, which indicates the presence of structural defects in the film. It has been shown that the microrelief of the CdTe growth surface is a criterion for the structural perfection of the layers and can be measured using an ellipsometer both at the early stages and during steady-state growth.

**Keywords:** molecular beam epitaxy, *in situ* ellipsometric control, CdTe, microrelief, growth defects.

DOI: 10.61011/SC.2023.06.57167.5278

## 1. Introduction

Currently, mercury-cadmium-telluride (MCT) is one of the most promising materials for the manufacture of infrared photodetectors (PD), both single and matrix [1]. One of the critical parameters for matrix PD is the uniformity of the electrophysical and optical properties of the material over the area. The most suitable method of manufacturing CMT that provides this requirement is the method of molecular beam epitaxy (MBE). The method makes it possible to produce large-area structures on substrates of the appropriate size, but at the same time a number of requirements are imposed on the substrates themselves. They should be structurally, chemically, optically and mechanically consistent with the CMT, the substrates should be large and inexpensive for mass production and compatible with electronic components of PD.

CdTe and CdZnTe substrates are attractive from the point of view of the convenience of growing CMT. But they have a number of disadvantages that limit their use in MBE technology, namely their price, heterogeneity of composition for CdZnTe, problems with surface cleanliness and their small size. The most optimal solution to the problem is hybrid silicon substrates with ZnTe and CdTe layers grown on them with a total thickness of several microns, which ensure the coordination of the parameters of the silicon lattice and the CMT layers [2].

The structural perfection of the grown CdTe layer is critically important for the subsequent growth of CMT on hybrid substrates. The formation of packaging defects, antiphase boundaries, and germinating dislocations is accompanied by the appearance of micro-roughness, which

limits the mobility of atoms on the surface of epitaxial growth and inevitably affects the quality of CMT layers [3]. It is necessary to maintain optimal growth conditions during the growth of buffer layers: the density of molecular beam flows and the substrate temperature. This requires continuous *in situ* control of crystal perfection during the growth process. The most optimal means of such control is ellipsometry. Ellipsometric measurements are very sensitive to the state of the surface, so the appearance of a microrelief, which is an indicator of defective growth, is detected at the very beginning of its development [4].

This paper presents studies of the growth process of ZnTe and CdTe buffer layers and ellipsometric techniques developed by us *in situ* to assess their crystal perfection and surface microrelief. The use of these techniques allows you to manage the growth process in real time, diagnose emerging problems in a timely manner, adjusting technological parameters if necessary in such a way as to avoid irreversible consequences. In some cases, the ellipsometer readings can serve as an indicator of abnormal deviations of the technological process and indicate the need for emergency measures.

## 2. Epitaxy equipment and analytical equipment

The growing of ZnTe and CdTe buffer layers was carried out in separate modules connected by a transport node for the transfer of samples without contact with air. The growth process was controlled by ellipsometers installed on each camera. The setup is described in more detail in [2].

To characterize the optical and structural properties of the buffer layers grown, *in situ* ellipsometers were used (laser ellipsometer in the ZnTe growth chamber and spectral ellipsometer for CdTe cultivation). The spectral ellipsometer, operating on a two-channel static circuit [5], had a range from 350 to 1000 nm. The long-term stability of measuring ellipsometric parameters is no worse than  $\delta\Psi = \delta\Delta = 0.01^\circ$ . The measurement time of one spectrum is 30 s. The ellipsometer operated in tracking mode at a fixed wavelength with a polling period of 20 s for registering fast-flowing processes. An ellipsometer similar in functionality, but with an extended spectral range of 250–1000 nm, was also used for *ex situ* studies.

The surface profile  $h(x, y)$  was measured using profilometer *S neox* by Sensofar Metrology. We used the interferometry method with coherent scanning. The vertical resolution of less than one nanometer is ensured for all numerical apertures owing to the application of this method. The lateral resolution was less than a micrometer. The algorithms used in this method allow you to use all available magnifications to profile objects with the same height resolution.

A scanning probe microscope Solver P47 Pro was also used to measure the relief, measurements were carried out in semi-contact mode

### 3. Optical properties of ZnTe layers

Figure 1 shows the spectra of the optical constants of ZnTe films with a thickness of 20 and 1080 nm, calculated from the results of *ex situ* ellipsometric measurements. The model „Si substrate/ZnTe layer/surface layer“ was used for the calculation. The surface layer describes the presence of natural oxide and roughness. The effective thickness of the surface layer was selected in such a way as to minimize the discrepancy between the experimental and calculated values of the parameter  $\Delta$  in the area of fundamental absorption of ZnTe. The calculations used the data of the directory [6]. The optical constants  $n, k$  for each wavelength were calculated by numerical solution of the ellipsometry equation for a given thickness  $d$  of the ZnTe layer, the value of which was determined from the condition that the absorption index in the transparency region was equal to zero (for thick films). The absorption index in the transparency region monotonically decreased in thin films with increasing wavelength, so the thickness was chosen from the condition that the absorption index was equal to zero at the right edge of the spectral range. Despite the fact that such a criterion does not guarantee the correct value of  $d$  and the absolute values of the calculated functions  $n(\lambda), k(\lambda)$ , we can see their characteristic features. So, the absorption edge of a thick film is characterized by a sharp jump  $k(\lambda)$ , as it should be in a straight-band semiconductor, while for a thin film ( $d = 20$  nm), the spectra of  $n(\lambda)$  and  $k(\lambda)$  are blurred near the absorption edge ( $\lambda_0 = 560$  nm), while the Urbach tail penetrates far into the transparency

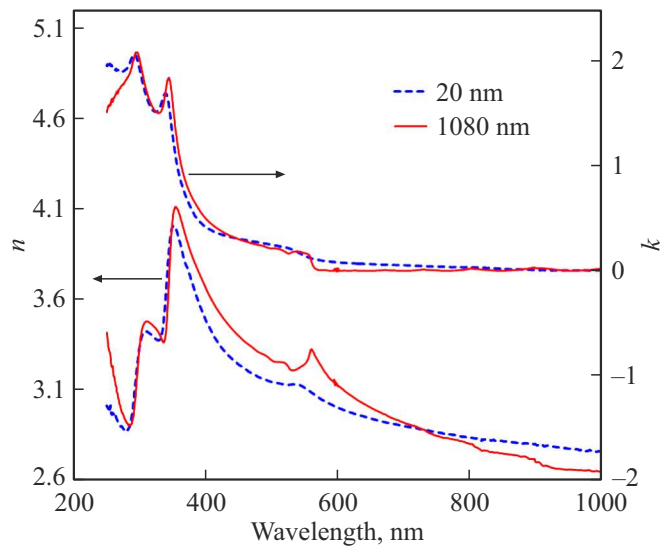


**Figure 1.** Spectra of optical constants  $n(\lambda)$  and  $k(\lambda)$  of ZnTe films grown on a Si substrate using the MBE method. The thicknesses of the films are shown in the inset of the figure.

region of the material, indicating the presence of optically active defects in the crystal structure [7]. A blurring of the structure of the spectra in the doublet region  $E_1/E_1 + \Delta_1$  is also observed in a thin film.

Experiments carried out in the process of debugging the technology showed that instead of growing a thick ZnTe layer, the density of crystal defects can also be minimized by growing a thick ( $\sim 5 \mu\text{m}$ ) CdTe layer on a thin ZnTe layer, which is more preferable for technological reasons. The application of CdTe to ZnTe leads to the overgrowth of residual defects and a decrease in their concentration near the surface to a level acceptable for obtaining defect-free CMT layers with high electrophysical parameters. This was the final criterion for optimizing thicknesses.

### 4. Characterization of structural properties of CdTe buffer layers

The characteristic of the structural quality of CdTe buffer layers is its optical constants — refractive index spectra  $n$  and absorption  $k$ . The highest sensitivity of the spectra to defects and microrelief is manifested near the critical points, which are located in the spectral region of 300–400 nm. The principle of „biggest is best“ is implemented — the smoothest surface corresponds to the largest value of the pseudo-dielectric function  $\langle \epsilon_2 \rangle$  [8]. However, in our case, the application of this criterion is limited by a decrease in the light intensity in the UV region, where the critical point  $E_1$  is available for measurements, due to the overgrowth of the I/O windows of radiation by the scattering products of molecular beams. As for the analysis of CdTe optical constants near the absorption edge, this involves solving the inverse ellipsometry problem and is not feasible in real time.

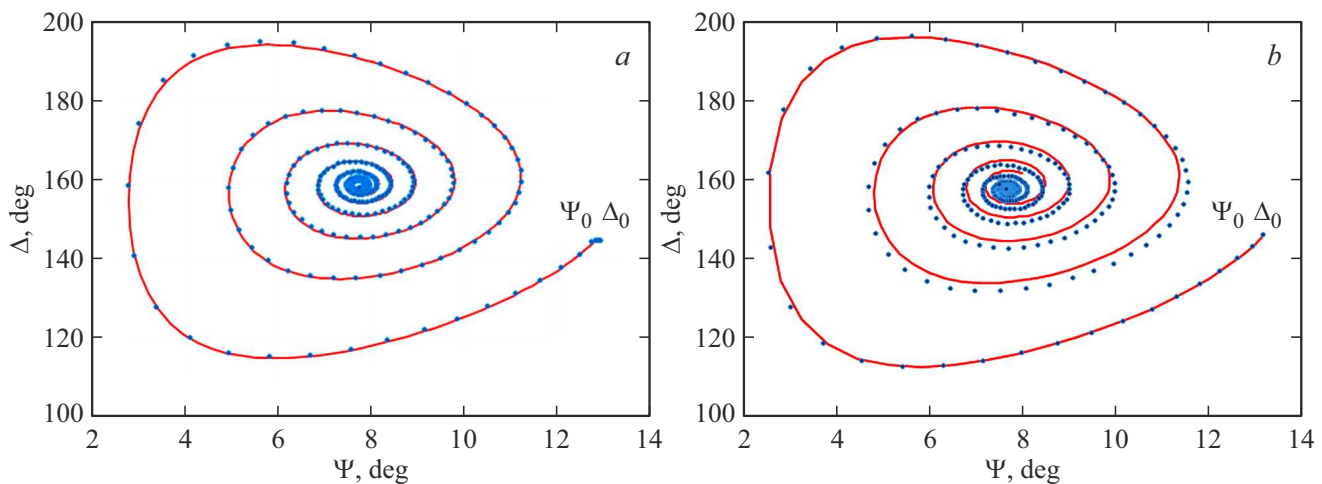


**Figure 2.** The trajectory of ellipsometric parameters at the initial stage of growth of the CdTe buffer layer: *a* — for a sample with a „smooth“ surface ( $h_{av} < 4$  nm), *b* — for a sample with a microrelief ( $h_{av} = 16$  nm). Points — experiment, solid curve — calculation. (A color version of the figure is provided in the online version of the paper).

An alternative criterion for assessing the crystallinity of the material and surface quality is the value of the parameter  $\Delta$  in the region of normal dispersion between the critical points  $E_0$  ( $\lambda \approx 860$  nm) and  $E_1$  ( $\lambda \approx 370$  nm). Roughness is taken into account when calculating the parameters  $\Psi$ ,  $\Delta$  by adding a surface layer to the structure, the optical constants of which are determined by the Bruggeman model [9]. The presence of such a layer for cadmium telluride with a refractive index in the specified spectral region  $n \approx 3$  will always lead to a decrease in the parameter  $\Delta$ . It is important that this decrease can be observed in dynamics from the first minutes of growth. Figure 2 shows the trajectories of ellipsometric parameters measured at the wavelength  $\lambda = 633$  nm for two samples at the initial stage of growth: CdTe221219 (*a*) and CdTe221220 (*b*). The experimental points in both cases describe a spiral curve that collapses to the limit point as the thickness increases. The solid line shows the results of the calculation using the „effective substrate/CdTe layer/surface layer“ model. The parameters of the effective substrate [10] are determined by the initial values  $\Psi_0$ ,  $\Delta_0$ . Optical constants of the CdTe layer can be selected for the CdTe221219 sample and the thickness of the surface layer, which ensure a good match of the calculated curve with the experiment. At the same time, the optical constants of the layer  $n = 3.146$  and  $k = 0.25$  obtained as a result of fitting are close to the optical constants of the perfect CdTe [6] crystal. The thickness of the surface layer  $d_r$  describing the microrelief is 0.9 nm.

For the CdTe221220 sample, it is not possible to select the structure parameters so that the entire experiment can be described. A good coincidence of the calculated curve with the experiment is observed at the same values of  $n$ ,  $k$ ,  $d_r$  as indicated above at the first turn of the spiral, however, the experimental points shift down the axis  $\Delta$  relative to the calculated trajectory with further growth. It is necessary to set  $d_r = 1.3$  nm to coordinate the experiment

with the calculation at the last turns of the spiral. This indicates the progressive development of micro-roughness and coarsening of the surface. As a rule, such samples have a more significant relief after the completion of growth.

Line-by-line measurements using the profilometer showed that the rms elevation of the relief  $h_{av} = \sqrt{\langle h \rangle^2}$  of CdTe221219 sample does not exceed 3 nm, while in case of CdTe221220 sample it does not exceed  $h_{av} > 10$  nm. Thus, the development of the microrelief at the initial stage determines the degree of roughness of the grown buffer layer. It should be noted that the thickness of the surface rough layer determined from ellipsometric measurements  $d_r$  and the height measured by the profilometer  $h_{av}$  cannot be compared quantitatively, since they describe different relief scales. Ellipsometric measurements are sensitive to lateral relief dimensions with a scale smaller than the wavelength, while measurement statistics on the profilometer operate with dimensions that are commensurate and larger than the wavelength. Nevertheless, the above comparison, as well as separately performed studies, show that there is a statistical correlation between the parameters  $d_r$  and  $h_{av}$ .

The measurements made using the profilometer were compared with the data obtained using the atomic force microscope. Figure 3 shows the results of this comparison — mean square values of height calculated from the results of measurements by two methods with one-dimensional scanning of an area with a length of  $50 \mu\text{m}$  on several CdTe films with varying degrees of roughness. There is a good correlation of the results. This comparison shows that, despite the twofold difference in absolute values, the data obtained on the profilometer qualitatively characterize the size of the microrelief.

Another important result, which is confirmed by the data of Figure 2 — is the absence of a transition layer between ZnTe and CdTe. Indeed, the experimental points fall on the

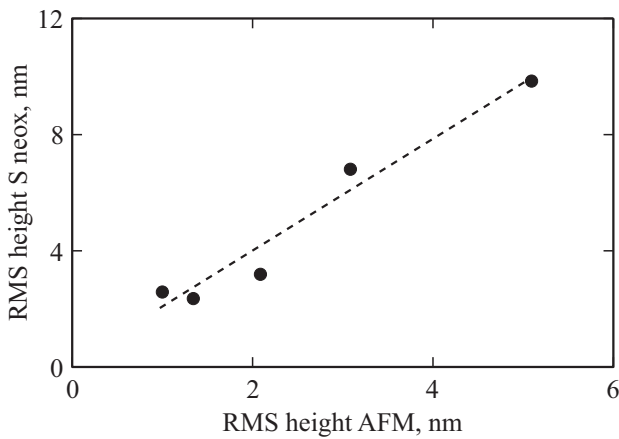


**Figure 3.** Comparison of the root-mean-square values of the relief height calculated from the results of measurements of five CdTe samples with an atomic force microscope and on a profilometer S neox (symbols). Dotted line — trend line.

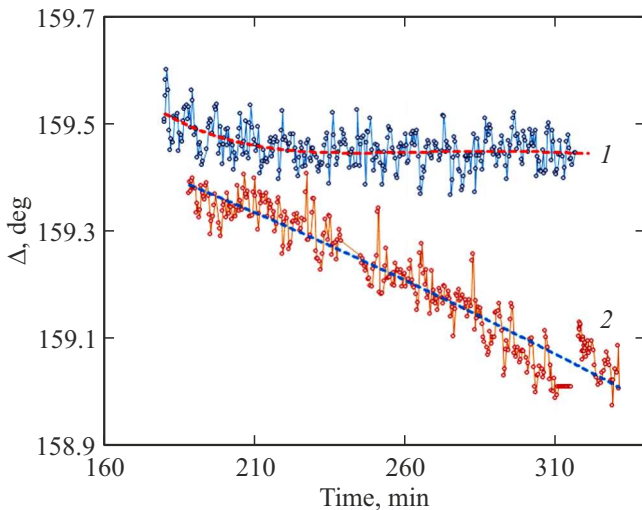


**Figure 4.** Dependences of the parameter  $\Delta$  on the growth time at a wavelength of 633 nm for samples CdTe221219 (curve 1) and CdTe221201 (curve 2), measured after the interference oscillations are completed. The dotted line shows the trend lines of the experimental data.

calculated curve from the first seconds of growth, thereby demonstrating the presence of a sharp interface.

With further growth, when the thickness exceeds the depth of light penetration and the interference oscillations  $\Psi$  and  $\Delta$  disappear, the development of the relief still affects the magnitude of the phase parameter  $\Delta$  and leads to its decrease. Figure 4 shows the measured values  $\Delta$  of the CdTe growth time for two samples: CdTe221219 (curve 1) and CdTe221201 (curve 2). The value of  $\Delta$  of the CdTe221219 sample with a relatively smooth surface remained virtually unchanged during the entire epitaxy process, thereby demonstrating stable film growth. A monotonous drop of  $\Delta$  by  $\sim 0.4^\circ$  was observed in

CdTe221201 sample during its growth, which served as an indicator of the development of microrelief. Post-test measurements of this sample on a profilometer showed that  $h_{av} = 16$  nm.

When growing a photosensitive CMT layer on buffer layers similar to the CdTe221201 sample, further degradation of the growth surface is usually observed, a high density of V-defects, and the density of germinating dislocations reaches  $4 \cdot 10^7 \text{ cm}^{-2}$ . On the contrary, in the process of CMT epitaxy on a „smooth“ substrate (similar to the CdTe221219 sample), it is much easier to maintain a high value of the parameter  $\Delta$ . At the same time, layers with good characteristics grow, with a dislocation density at the level of  $(2-5) \cdot 10^6 \text{ cm}^{-2}$ , which are suitable for creating optoelectronic devices. The value of  $0.5^\circ$  can be considered to be a critical value of the drop of  $\Delta$  in the process of CdTe growth, distinguishing the CMT suitable for further epitaxy from the unsuitable ones.

There are a number of reasons that can lead to the progressive growth of microrelief. This may be a deviation from the optimal temperature regime, and a suboptimal ratio of the densities of the molecular flows of tellurium and cadmium, and the residual background pressure in the growth chamber. Additional information about the properties of buffer layers can be obtained from the spectra of ellipsometric parameters measured after the completion of growth. The most interesting area is the transparency of the material, where their interference oscillations are observed. Figure 5 shows such oscillations of the parameter  $\Delta$  for a series of samples grown sequentially over several days. The beginning of the oscillations occurs at the absorption edge, and their amplitude monotonically increases as they shift into the long-wave region. The increase of oscillations is described by the same envelope for samples CdTe221215, CdTe122216 and CdTe221219. The oscillation amplitude of samples CdTe221220 and CdTe221221 is noticeably smaller. The scope of interference oscillations depends on the magnitude of the absorption index in the CdTe

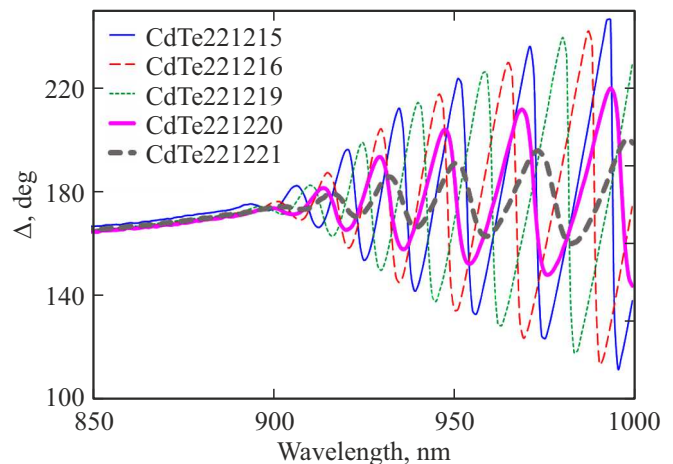


**Figure 5.** The spectra of the parameter  $\Delta$  for a series of samples grown under conditions of Cd deficiency.



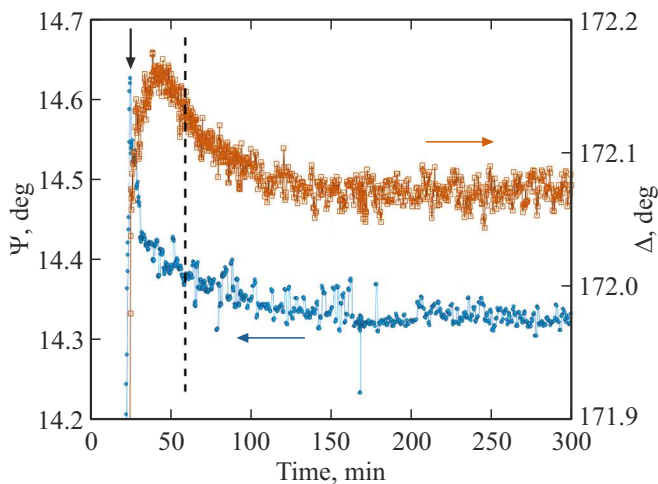


**Figure 6.** Changing the parameters  $\Psi$  and  $\Delta$  of the silicon plate during its heating and subsequent temperature relaxation. The vertical arrow shows the moment when the heater switches to stationary mode, the vertical dotted line corresponds to the time at which the growth of the CdTe layer begins.

layer. The decrease of amplitude may be associated with an increase of absorption on defects in the crystal structure, as was observed above for thin ZnTe layers. However, such a significant decrease of amplitude implies too high absorption. An alternative explanation of the observed effect is due to the heterogeneity of the layer thickness over the sample area. In this case, different thickness values fall into the area of the probing spot and the interference pattern is blurred.

In any case, a monotonous decrease in amplitude for two sequentially grown samples, as well as an observed increase in relief for CdTe221221 and CdTe221222 samples indicate a deviation from optimal growth conditions. The opening of the chamber showed that this was caused by the heterogeneity of the Cd flux density on the substrate surface due to the almost complete evaporation of the material loaded into the crucible. Thus, the appearance of microrelief and the observation of interference oscillations of ellipsometric parameters in the IR region with an abnormally small amplitude serve as an indicator of unfavorable growth and require preventive measures.

As already noted, the growth of a smooth surface is accompanied by a stable value of the parameter  $\Delta$ . However, in experiments of this kind, there is still a slight drop in the parameter  $\Delta$  by the value  $0.05\text{--}0.1^\circ$  (Figure 4, curve 1). In order to understand the reasons for this behavior  $\Delta$  and to find out whether or not this fall is due to a slight development of the microrelief, a test experiment was conducted. First of all, the hardware stability of the ellipsometer was investigated. To do this, a Si plate was loaded into the chamber and continuous measurements of its ellipsometric parameters were carried out at room temperature during the day. The ellipsometer demonstrated exceptionally high long-term stability: the standard deviation

of the parameters  $\Psi$  and  $\Delta$  from their average values was only  $0.0013^\circ$ . Then, all the technological operations that are performed to establish the temperature regime during CdTe epitaxy were performed with this plate, with the exception of the CdTe growth itself.

According to the technological regulations, before the CdTe growth, the Si/ZnTe structure quickly (within 400 s) heats up to the growth temperature. Due to the high heating rate, there is a slight overheating of the substrate. Therefore, after switching the heater power to stationary mode, we waited 30 minutes, during which, according to our ideas, temperature relaxation should occur.

Figure 6 shows the dependences of ellipsometric parameters  $\Psi$  and  $\Delta$ , measured during the described procedure: silicon heating and subsequent exposure. After reaching the maximum temperature and changing the heater mode (at  $t = 25$  min), the parameter  $\Psi$ , which is sensitive to temperature, changes during  $\sim 130$  min and relaxes to its stationary value. The moment corresponding to the beginning of growth in experiments with CdTe epitaxy is shown by a vertical dotted line. For 100 min after that, the parameter  $\Psi$ , and consequently, the temperature of the Si substrate continued to change slightly. According to the data of [11], the sensitivity of the parameter  $\Psi$  to a change in silicon temperature at a given angle of incidence ( $\varphi = 68.2^\circ$ ) is  $\Delta\Psi/\delta T = 2.7 \cdot 10^{-3}$  ang deg/ $^\circ\text{C}$ . The observed residual change of  $\Psi$  in the area to the right of the dotted line is  $0.05^\circ$  and corresponds to a temperature change of  $\sim 20^\circ\text{C}$ . Taking into account the temperature sensitivity of the parameter  $\Delta$  for CdTe  $d\Delta/dT = 2 \cdot 10^{-3}$  ang deg/ $^\circ\text{C}$  [12], we obtain that for a given wavelength and angle of incidence, the decrease is  $\Delta$  due to temperature relaxation should be  $\sim 0.04^\circ$ . This coincides in order of magnitude with what is observed for the curve 1 Figure 4 by decreasing  $\Delta$ . Thus, we can conclude that the drop of  $\Delta$  to  $0.05\text{--}0.1^\circ$  observed at the beginning of CdTe growth is not due to the development of the relief and not to hardware drift, but is due to the continued relaxation of the substrate temperature.

It is interesting to note that after switching the heater mode, the parameter  $\Delta$  continues to grow for some time and only after 15–20 min begins to fall. This type of change  $\Delta$  is associated with the thermal removal of the adsorbed layer (primarily water), which is present on the silicon surface, and was observed in the work of [13].

## 5. Conclusion

The growing of buffer layers of high crystal perfection is a prerequisite for the subsequent epitaxy of CMT and the production of layers that can be used to create devices. A reliable *in situ* control, which provides feedback in the technology of growing buffer layers is an indispensable condition for solving this problem. The conducted studies show that the ellipsometry method used for this purpose has a high sensitivity, allows you to characterize the growth

process in real time and timely monitor minor deviations from a given technological regime. One of the criteria for this deviation is the microrelief of the growth surface, which affects the value of the phase parameter  $\Delta$  and is easily detected by ellipsometric measurements. Using this criterion, it is possible to maintain optimal growth conditions and obtain high-quality buffer layers suitable for CMT epitaxy.

### Acknowledgments

The authors express their gratitude to A.I. Komonov for carrying out measurements on an atomic force microscope.

### Funding

This study was financially supported by a grant from the Ministry of Science and Higher Education of the Russian Federation No. 075-15-2020-797 (13.1902.21.0024).

### Conflict of interest

The authors declare that they have no conflict of interest.

### References

- [1] *Mercury Cadmium Telluride. Growth, Properties and Applications*, ed. by P. Capper and J. Garland (Wiley, 2011).
- [2] Y.G. Sidorov, S.A. Dvorestkiy, V.S. Varavin, N.N. Mikhailov, M.V. Yakushev, I.V. Sabinina. *FTP*, **35**, 1092 (2001). (in Russian).
- [3] J. Zhao, Y. Chang, G. Badano, S. Sivananthan, J. Markunas, S. Lewis, J.H. Dinan, P.S. Wijewarnasuriya, Y. Chen, G. Brill, N. Dhar. *J. Electron. Mater.*, **33**, 881 (2005).
- [4] K.K. Svitasev, V.A. Shvets, A.S. Mardezhov, S.A. Dvoretiskii, Yu.G. Sidorov, V.S. Varavin. *ZhTF*, **65** (9), 110 (1995). (in Russian).
- [5] E.V. Spesivtsev, S.V. Rykhlytskii, V.A. Shvets. *Avtometriya*, **47** (5), 5 (2011). (in Russian).
- [6] S. Adachi. *Optical constants of crystalline and amorphous semiconductors. Numerical data and graphical information* (Kluwer Academic Publishers, 1999).
- [7] Y. Chang, G. Badano, J. Zhao, Y.D. Zhou, R. Ashokan, C.H. Grein, V. Nathan. *J. Electron. Mater.*, **33**, 709 (2004).
- [8] D.E. Aspnes, A.A. Studna. *Phys. Rev. B*, **27**, 985 (1983).
- [9] D. A. G. Bruggeman. *Annalen der Physik*, **416** (7), 636 (1935).
- [10] V.A. Shvets. *Opt. i spectr.*, **107**, 822 (2009). (in Russian).
- [11] X. Xu, C.P. Grigoropoulos. *Int. J. Heat Mass Transfer*, **36**, 4163 (1993).
- [12] D.V. Marin, V.A. Shvets, I.A. Azarov, M.V. Yakushev, S.V. Rykhlytskii. *Infr. Phys. Technol.*, **116**, Article 103793 (2021).
- [13] E.V. Spesivtsev, S.V. Rykhlytsky, V.A. Shvets, S.I. Chikichev, A.S. Mardezhov, N.I. Nazarov, V.A. Volodin. *Thin Sol. Films*, **455**, 700 (2004).

*Translated by A.Akhtyamov*